

1  
2 **Vectorchip: Microfluidic platform for highly parallel bite by bite**  
3 **profiling of mosquito-borne pathogen transmission**

4 Shailabh Kumar<sup>†1</sup>, Felix J. H. Hol<sup>†1, 2, 3</sup>, Sujit Pujhari<sup>4</sup>, Clayton Ellington<sup>1</sup>, Haripriya Vaidehi  
5 Narayanan<sup>1</sup>, Hongquan Li<sup>5</sup>, Jason L. Rasgon<sup>4</sup>, Manu Prakash<sup>1,\*</sup>

6 1 Department of Bioengineering, Stanford University, Stanford, CA, USA

7 2 Insect Virus Interactions Unit, Department of Virology, Institut Pasteur, Paris, France

8 3 Center for Research and Interdisciplinarity, U1284 INSERM, Université de Paris, Paris, France

9 4 Department of Entomology, The Center for Infectious Disease Dynamics, and the Huck  
10 Institutes of The Life Sciences, The Pennsylvania State University, University Park, PA, USA

11 5 Department of Electrical Engineering, Stanford University, Stanford, CA, USA

12 † these authors contributed equally

13 Corresponding author: [manup@stanford.edu](mailto:manup@stanford.edu)

14 **Abstract**

15 Mosquito bites transmit a number of human pathogens resulting in potentially fatal diseases includ-  
16 ing malaria, dengue, chikungunya, West Nile encephalitis, and Zika. Although female mosquitoes  
17 transmit pathogens via salivary droplets deposited during blood feeding on a host, very little is  
18 known about the genomic content of these nanoliter scale droplets, including the transmission dy-  
19 namics of live pathogens. Here we introduce *Vectorchip*, a low-cost, scalable microfluidic platform  
20 for molecular interrogation of individual mosquito bites in a high-throughput fashion. An ultra-  
21 thin PDMS membrane coupled to a microfluidic chip acts as a biting interface, through which  
22 freely-behaving mosquitoes deposit saliva droplets by biting into isolated arrayed micro-wells en-  
23 abling molecular interrogation of individual bites. By modulating membrane thickness, the device  
24 enables on-chip comparison of biting capacity and provides a mechanical filter allowing selection  
25 of a specific mosquito species. Utilizing *Vectorchip*, we show on-chip simultaneous detection of  
26 mosquito DNA as well as viral RNA from Zika infected *Aedes aegypti* mosquitoes – demonstrating  
27 multiplexed high-throughput screening of vectors and pathogens. Focus-forming assays performed  
28 on-chip quantify number of infectious viral particles transmitted during mosquito bites, enabling  
29 assessment of active virus transmission. The platform presents a promising approach for single-  
30 bite-resolution laboratory and field characterization of vector pathogen communities, to reveal the  
31 intricate dynamics of pathogen transmission, and could serve as powerful early warning artificial  
32 “sentinel” for mosquito-borne diseases.

## 33 Introduction

34 Mosquito-borne pathogens and diseases including malaria, dengue, chikungunya, West Nile en-  
35 cephalitis, Japanese encephalitis, and Zika afflict more than 300 million individuals every year,  
36 resulting in more than 500,000 deaths [1]. As a result of increasing environmental pressures and  
37 human migration, these diseases are expected to continuously increase their geographical range,  
38 placing more than 50% of the world human population at risk within decades [2,3]. To curb this  
39 crisis, we urgently need new tools to expand our understanding of mosquito-pathogen commu-  
40 nities and transmission mechanics. In addition, expanding the scale of surveillance of infectious  
41 mosquito species and associated pathogens is critical for deployment of better-informed preventa-  
42 tive measures in communities.

43 Molecular analysis of genomic material, proteins, or metabolites remains the gold standard for  
44 the detection and study of mosquito-pathogen communities in various settings. In order to obtain  
45 molecular samples for field ecology, mosquitoes are typically collected through different modali-  
46 ties of traps [4,5] or via human landing catches, which remain an ethically questionable method for  
47 gathering data [6–8]. These resource-intensive sample collection strategies commonly suffer from  
48 a limited scale of operation. As a result, severe undersampling of mosquito and pathogen popula-  
49 tions remains a major concern around the globe [9]. In addition, molecular analysis of mosquitoes  
50 in the lab or field is usually performed using either (i) whole body sampling of mosquitoes by  
51 homogenizing them [10], (ii) analysis of mosquito saliva after extraction of salivary glands [11], or  
52 (iii) forced mosquito salivation [12] to determine the prevalence of pathogens in mosquito popula-  
53 tions. In addition to requiring sample preparation of mosquitoes, these methods do not represent  
54 actual biting events thus providing limited information about the transmission dynamics such as  
55 infectious viral load in bites. More recently, alternative modes of sample collection exploiting e.g.  
56 sugar feeding or excreta have been proposed [13–17], but similarly do not simulate biting events,  
57 cannot differentiate between pathogens in saliva vs gut, provide population level (i.e. pooled)

58 information with limited scope of improvement in resolution, and cannot quantify live viruses.  
59 A significant gap exists in our knowledge which requires novel tools to (i) quantitatively track  
60 the dynamics of pathogen transmission directly from single mosquito bites, and (ii) improve the  
61 throughput of molecular profiling of mosquito populations to boost surveillance strategies.

62 High-throughput molecular interrogation of saliva from mosquito bites can provide a new window  
63 into the dynamics of vector-borne disease transmission. Quantification of genomic content of sali-  
64 vary droplets and pathogen transmission directly from bites can help shed light on the dynamics  
65 of transmission at bite-by-bite resolution [18]. At the same time, parallel profiling of multiple  
66 biting events can lead to highly accelerated sampling of large vector populations in the field. Cur-  
67 rently, an important barrier to developing such methods is the lack of a suitable vector-device  
68 interface. Membrane materials such as parafilm and animal casings typically used to interface  
69 with mosquitoes [19–21], lack the thermal and chemical compatibility needed to perform nucleic  
70 acid amplification, cell culture, and integration with microfluidic device manufacturing practices.  
71 As a result, it is imperative to look for novel materials and protocols that can change the landscape  
72 of vector-pathogen diagnostics.

73 In this work, we demonstrate *Vectorchip* - a microfluidic platform for molecular diagnostics of indi-  
74 vidual salivary droplets from mosquitoes allowing on-chip detection of mosquito DNA, viral RNA,  
75 and infectious viral particles directly from mosquito bites. This is enabled by a new fabrication  
76 strategy, resulting in reaction-ready, skin-mimic polydimethylsiloxane (PDMS) membranes which  
77 allow mosquitoes to bite and feed through them. We investigate the biting of various mosquito  
78 species using this chip, discovering biomechanical differences in biting capacity which can be  
79 used to create species-selective feeding barriers. Saliva from the biting activity of mosquitoes on  
80 *Vectorchips* is autonomously collected in individually isolated reaction chambers. Nucleic acid  
81 amplification assays conducted on-chip indicate that mosquito DNA and viral RNA are released  
82 during these biting events enabling identification of both the vector and pathogen. Finally, we

83 show direct quantification of live, infectious viral particles from mosquito bites using focus form-  
84 ing assays (FFA) on chip, enabling interrogation of pathogen transmission through direct profiling  
85 of individual mosquito bites at high throughput.

## 86 **Results**

### 87 **Device design and fabrication:**

88 Vectorchips with integrated PDMS elastomer membranes were fabricated using a combination of  
89 laser patterning and soft lithography. We selected PDMS as the material of choice due to its low  
90 cost, biocompatibility, optical transparency, and chemical stability. PDMS-based devices can be  
91 fabricated using reproducible and scalable fabrication techniques [22]. Such devices have rou-  
92 tinely been used for molecular analysis of small sample volumes using microfluidics [23], and are  
93 compatible with molecular assays and cell cultures [24, 25]. We used laser patterning to create  
94 open-ended arrayed compartments in PDMS for saliva capture (Fig. 1a-d). A thin elastomeric film  
95 was formed by spin-coating uncured PDMS over a flat silicon surface. We obtained membrane-  
96 integrated devices after plasma-induced PDMS-PDMS bonding of the laser-patterned array with  
97 the elastomeric film (Fig. 1e). Detailed steps describing chip development are included in the  
98 methods section. The fabrication process is extremely versatile and allows for user-defined varia-  
99 tion in the size and density of the individual compartments. We were able to fabricate chips with  
100 hole diameters ranging from 150  $\mu\text{m}$  to 1 cm (Fig. S1) showing the scales of operation for the  
101 laser-ablation process while maintaining membrane stability. Additionally, the membrane can be  
102 easily integrated with fluidic networks for direct interfacing with mosquito bites, enabling assays  
103 involving on-chip fluid exchange (Fig. 1f). The microfluidic compartments on the chips can hold  
104 feeding media such as blood or sugar water (Fig. 1g), collect saliva during biting events, and act  
105 as isolated reaction chambers for molecular assays.

## 106 **Mosquito-chip interactions**

107 We tested the ability of mosquitoes to pierce through the PDMS membranes. Mosquitoes were  
108 attracted to the chips using heat as a guiding cue. We placed a camera above the chip and ob-  
109 served stylet insertion through 1.6  $\mu\text{m}$  thick PDMS membranes (Fig. 2a, Supp. Movie 1,2 , Note:  
110 thickness of the PDMS membrane at 1.6  $\mu\text{m}$  was selected by maximum spin speed available at  
111 the time of these experiments). Abdominal engorgement in mosquitoes was observed after bit-  
112 ing, indicating that mosquitoes can successfully feed through these membranes. Four species of  
113 mosquitoes were tested (*Aedes aegypti*, *Aedes albopictus*, *Culex tarsalis*, *Culex quinquefasciatus*)  
114 and demonstrated successful probing and feeding through 1.6  $\mu\text{m}$  thick PDMS membranes.

115 We also examined whether the membrane thicknesses can be engineered to selectively prevent  
116 biting of some species while letting others feed. We loaded the laser-patterned microfluidic com-  
117 partments with blood and warmed the chips to attract mosquitoes (Fig. S2, Supp. Movie 3).  
118 We considered biting to be “off” when none of mosquitoes in the cage demonstrated abdominal  
119 engorgement within 30 minutes since start of the experiment. Tests were performed with *Aedes*  
120 *aegypti* ( $\sim 45$  mosquitoes per cage) and *Culex tarsalis* ( $\sim 25$  mosquitoes per cage) while varying  
121 the thickness of the PDMS membrane from 900 nm to 100  $\mu\text{m}$ s. We observed significant differ-  
122 ences in the biting ability of the two species, where complete inhibition of feeding in *Aedes aegypti*  
123 was observed with membrane thickness at or greater than 15  $\mu\text{m}$ s (Supp. Movie 4, 5). In contrast,  
124 complete inhibition of feeding with *Culex tarsalis* was observed for membranes that were 100  $\mu\text{m}$ s  
125 thick (Fig. 2b). Even though a larger population of *Aedes aegypti* were available to feed from  
126 the chips, their biting strength appeared to be inferior to *Culex tarsalis*. This remarkable differ-  
127 ence in probing capacity of these two species has not been reported earlier. While some studies  
128 have focused on understanding the biting mechanics of a single mosquito species (*Aedes aegypti*  
129 or *Aedes albopictus*) [26,27], we are not aware of any study which looks at the difference in biting  
130 strength between different species and the evolutionary or biomechanical differences involved in  
131 this variation. This intriguing biomechanical phenomenon can be advantageous by deploying de-

132 vices where membranes of desired thickness can act as species-selective filters, providing a means  
133 to better track highly relevant species and pathogens in the field.

134 In order to extract molecular information from mosquito bites, the chip aims to exploit the release  
135 of saliva during probing and biting events. The release of salivary droplets can be visualized  
136 using fluorescence imaging of mosquitoes fed on rhodamine-labeled sugar water, which renders  
137 the saliva fluorescent (Fig. 2e, Supp. Movie 6). Time sequences (Fig. 2f) show magnified images  
138 of three locations on a membrane surface where short probing activity results in deposition of  
139 salivary droplets. These salivary droplets house several biomarkers in the form of mosquito salivary  
140 proteins [28], active pathogens, mosquito cells and/or nucleic acids that can be used for their  
141 identification [12, 18, 29].

#### 142 **Tracking dynamics on-chip**

143 A major consideration for biting based diagnostics would be the ability to sample either the whole  
144 population or individual mosquitoes. The relationship between number of mosquitoes interacting  
145 with each isolated reaction chamber should depend on the number of mosquitoes in the cage, the  
146 time of interaction, number of wells, and the area of the chip. It is possible that the feeding media  
147 also affects the number of biting events performed by a female mosquito. We utilize sucrose as the  
148 feeding media since it is a diet source that does not inhibit polymerase chain reaction (PCR) assays  
149 and therefore will limit the analysis to this feeding solution. In order to perform sucrose biting  
150 assays for molecular diagnostics, we filled the wells with 10% sucrose, and covered the open side  
151 of the chip with a glass slide. A resistor which acts as a heat source was placed atop the glass  
152 slide and the chip-resistor assembly was placed on top of the mesh ceiling of a mosquito cage. A  
153 part of the chip was protected by a paper tape such that mosquitoes cannot bite into the membrane.  
154 The area of the chip protected by tape serves as negative control for the biting assays. A camera  
155 was placed on the bottom of the cage to track and record mosquito activity on chip (Fig. S3).  
156 Image recognition algorithms were used to analyze the obtained images and track the presence

157 and movement of mosquitoes on the chip (Fig. 3a-d, Supp. Movie 7). Tracking data reveals the  
158 dynamics of mosquito-chip interactions indicating the trajectories followed by mosquitoes and the  
159 time spent by mosquitoes at different spots on the chip. Regions with non-overlapping trajectories  
160 reveal the areas which are most-likely to be probed by a single mosquito (Fig. 3d).

161 On-chip location and tracking dynamics for mosquitoes on different chips is shown in Fig. 3e-g and  
162 Fig. S3. Three cases are demonstrated - i) over a short time period and low mosquito density, no  
163 overlap between any of the trajectories is found (Fig. 3e). ii) Increasing the time of interaction, we  
164 can simultaneously obtain both individual tracks and pooled probe data (Fig. 3f). iii) An extended  
165 interaction time between mosquito population and the chip results in complete overlap between  
166 trajectories (Fig. 3g). The results indicate that by modulating the time of interaction between the  
167 mosquito population and the chip, the user can control the degree of probing experienced by the  
168 chip. As an example, for a chip where there is no overlap between trajectories, every probed well  
169 should provide single mosquito-resolution data.

170 While the tracking of mosquitoes on chip provides information about mosquito locomotion and  
171 time spent over different areas of the chips, fluorescent salivary emission can be used as a means  
172 to gauge the extent of probing over different regions of the chip. We quantified the number of  
173 spots seen in different wells of the PDMS chip by using fluorescent scans of the chip before and  
174 after biting (Fig. 3h, i). No spots were observed in the negative control region where access was  
175 blocked to mosquitoes. Several spots were observed on the open areas of the chip, with several  
176 wells indicating that they have been bitten single time. These datasets indicate that the *Vectorchip*  
177 provides opportunities to obtain data at both the individual bite level as well as pooled-profiling of  
178 multiple bites.

### 179 **PCR diagnostics on-chip**

180 We selected devices with PDMS membrane thickness of 1.6  $\mu\text{m}$  and well diameter of 1.75 mm as  
181 the first prototype to perform molecular analysis of salivary samples. These well dimensions were

182 amenable with manual pipetting while providing a dense array of 150 independent reactions per  
183 chip (within a chip area of 5 cm × 2.5 cm ).

184 Detection of mosquito mitochondrial DNA (mtDNA) and RNA from viruses in saliva was per-  
185 formed using on-chip PCR with end-point fluorescence readout. A detailed protocol for perform-  
186 ing PCR in *Vectorchips* is provided in the Methods section and Supporting Information file (Fig.  
187 S4). We tested the efficiency of PCR amplification in *Vectorchips* by manually loading a known  
188 concentration of DNA and RNA into the reaction wells (Fig. 4a-c). We performed the PCR for 42  
189 cycles and detect DNA amplification from approximately 5 DNA copies in 4 μL of reaction mix  
190 (~ 1 copy/μL) (Fig. 4b). Simultaneously for Zika reverse transcription-PCR (RT-PCR), viral RNA  
191 detection was successfully demonstrated from approximately 150 RNA copies in 4 μL of reaction  
192 mix (Fig. 4c). We verified the performance of end-point PCR in vectorchips by running reactions  
193 with identical reagents, volumes and conditions in 96 well plates. Both qPCR amplification curves  
194 and end point fluorescence information was obtained from the well plates. The reactions were  
195 tested in DI water and also in the presence of dried sucrose (10%) to ensure that amplification  
196 response correlated well with manually spiked concentrations and the presence of sucrose did not  
197 inhibit the reactions (Fig. S5(a,b)).

198 The chips were allowed to be probed by mosquitoes for 20-45 minutes. While testing uninfected  
199 mosquitoes, PCR assays were performed on-chip for detecting the presence of mosquito DNA in  
200 deposited salivary droplets. Fig. 4d-e shows the tracking data and PCR detection of mtDNA for a  
201 chip which was placed on a cage with 75 uninfected *Aedes aegypti* females for 45 minutes. Areas  
202 highlighted in green were protected by a paper tape such that mosquitoes cannot probe them and  
203 serve as negative controls. The tracking and PCR data obtained from the chip indicate significant  
204 locomotive activity of the mosquitoes on-chip, and detection of mosquito DNA in wells. Multiple  
205 experiments indicate that a subset (3 - 12%, n = 6) of the wells where mosquitoes are active test  
206 positive for presence of mosquito DNA (Fig. 4f). The rate of false positives obtained from wells



207 not accessible to mosquitoes was very close to zero (0.23%, n = 6). In order to further validate  
208 the rate of detection of mosquito DNA on *Vectorchips*, we performed a biting assay using a 96  
209 well plate loaded with agarose and covered with a parafilm membrane. We recorded the tracking  
210 and DNA amplification response from uninfected mosquito bites on the well plate (Fig. S5(c,d)).  
211 Around 15% of the wells where mosquitoes were active tested positive for presence of mosquito  
212 DNA, which is close to the fractions observed on vectorchips. Since mosquito DNA can only be  
213 detected in a subset of wells showing mosquito activity, this suggests that the presence of detectable  
214 levels of mosquito DNA in saliva is a noisy physiological process, likely dependent on multiple  
215 variables such as duration of feeding and time of last bite. It is furthermore important to note that  
216 our tracking algorithm only detects the presence of mosquitoes, but does not provide information  
217 regarding if a well was bitten or not.

218 Fig. 4h shows results obtained when *Aedes aegypti* infected with Zika virus [30] interacted with  
219 the chip for 20 minutes. We subsequently performed RT-PCR assay on the chip demonstrating that  
220 *Aedes aegypti* mtDNA and ZIKV RNA can be detected in 24/118 and 37/118 wells, respectively.  
221 We summarize the detection rates of mosquito DNA and Zika RNA for three assays performed  
222 with ZIKV-infected mosquitoes in Fig. 4i. Interestingly, not all wells positive for ZIKV RNA show  
223 positive for mosquito DNA and vice versa, highlighting the stochastic composition of bite-derived  
224 saliva droplets. A higher fraction of wells (mean  $\sim 22\%$ , n = 3) showed positive for ZIKV RNA  
225 as compared to mosquito mtDNA (mean  $\sim 17\%$ , n = 3), indicating a higher prevalence of viral  
226 genomic material in vector saliva as compared to mosquito mtDNA. Detection of mosquito DNA  
227 and virus RNA in these assays demonstrates the capacity of this tool towards the identification of  
228 mosquito and pathogen species directly from mosquito bites on-chip.

### 229 **Detection of infectious viral particles directly from bites**

230 While PCR-based end-point assays are an important strategy for multiplexed detection of vectors  
231 and pathogens in various settings, they cannot determine the presence or concentration of infectious

232 virus particles in bites. Detection of infectious pathogen load in mosquito bites is important to  
233 understand the vector competence of mosquito-pathogen systems and its dependency on factors  
234 such as local climate, mosquito physiology [31], and presence of endosymbionts (e.g. *Wolbachia*)  
235 [32, 33]. Typical methods to measure vector competence rely on manual “forced salivation” of  
236 individual mosquitoes [10], where the viral loads may differ from biting events. We tested the  
237 *Vectorchip* to perform focus forming assays (FFA) and detect infectious viral particles directly as  
238 a result of mosquito bites on chip (Fig. 5).

239 The wells were filled with cell culture media (Dulbecco’s modified eagle medium - DMEM). The  
240 efficiency of FFA on-chip was tested initially using manual spiking of viral particles into *Vec-*  
241 *torchips* (Fig. S6). In order to perform biting assays, *Aedes aegypti* mosquitoes were infected  
242 with Mayaro virus, an emerging zoonotic pathogen which causes a dengue like disease [34]. The  
243 mosquitoes were able to bite through the membrane into the wells and transfer live Mayaro vi-  
244 ral particles directly into the cell culture medium (Fig. 5a). These viral particles then infect a  
245 monolayer of vero cells cultured on the PDMS membrane. These infections can be identified via  
246 fluorescent antibodies specific to viral envelope proteins (Fig. 5c). Each fluorescent patch (focus)  
247 is attributed to infections transmitted by a single viral particle. Foci counted on two sample chips  
248 can be seen in Fig. 5d. No foci were visible from negative control samples. The distribution  
249 of viral foci on the chips indicate the heterogeneity of infectious particle dose in mosquito bites.  
250 The data in Fig. 5 demonstrate the suitability of using the *Vectorchip* to probe the transmission of  
251 infectious viral particles.

## 252 Discussion

253 We demonstrate a novel microfluidic device integrated with a PDMS “artificial skin” membrane  
254 for molecular diagnostics of individual mosquito bites on a chip. The device permits user-desired

255 modifications in chip design as well as more than two orders of magnitude variation in reaction  
256 chamber volume for performing molecular analysis. The elastomer membrane is compatible with  
257 scalable device fabrication, microfluidic integration, nucleic acid amplification assays, as well  
258 as cell culture assays, allowing multimodal interrogation of mosquito bites on chip. Interfacing  
259 mosquito bites with fluidic channels provide the potential of using this device with integrated  
260 vascular pathways or particle traps to study transport and subsequent infection dynamics of ex-  
261 pectorated pathogens in a user-controlled environment. As compared to previous methods, the  
262 *Vectorchip* uniquely allows quantitative interrogation of mosquito bites on a chip, which may an-  
263 swer questions such as the genomic diversity of bites, transmission dynamics of pathogens in bites,  
264 and enable high throughput diagnostics of large mosquito populations at single bite resolution .

265 We tested our devices with four mosquito species and all were able to probe through ultrathin  
266 PDMS membranes (thickness 1.6  $\mu\text{ms}$ ) demonstrating the ability of this device to interface with  
267 variety of vectors. Furthermore, our novel fabrication strategy permits us to engineer the “skin  
268 characteristics” such as thickness and stiffness. We discover that different species of mosquito can  
269 display significant variation in their biting strength, the biomechanical basis for which remains  
270 an intriguing question. This variation in probing capacity provides an opportunity to perform  
271 mechanical species selection for on-chip sample collection by careful engineering of the membrane  
272 thickness and stiffness. This observation also provides opportunities towards examining the biting  
273 capacity in different mosquito species and if there exists an evolutionary relationship of the biting  
274 ability with their preferred prey species.

275 We also utilize on-chip tracking of mosquito activity to demonstrate that varying the experimental  
276 parameters including chip design and number of mosquitoes can allow collection of bite data from  
277 the population as a pool or from individual bites. While population data can broadly indicate the  
278 presence of infectious agents in the community, individual bite statistics can help explore these  
279 phenomena at a higher (bite-by-bite) resolution.

280 The *Vectorchip* aims to significantly reduce the manual labor, time, and risk associated with cap-  
281 ture, individual segregation and sample extraction from individual mosquitoes as traditionally prac-  
282 ticed. Reaction in miniaturized chambers reduces the cost of molecular assays - chips used in this  
283 report (1.75 mm diameter) performed PCR reactions at 30 ¢per reaction chamber which is approx-  
284 imately 5× lower than current single mosquito homogenization assays. We also fabricated further  
285 miniaturized device designs with smaller well diameters, which can provide a 100× reduction in  
286 individual reaction volumes and lower the cost per-assay by two orders of magnitude (<1 ¢per  
287 reaction).

288 We detect that biting mosquitoes release their DNA on chip, which can be used to identify their  
289 species as well as targeted genetic mutations. Detection of these genetic signatures can be used  
290 for monitoring the spread of native or invasive mosquito species globally, insecticide resistance  
291 in mosquitoes, or tracking the range of gene-drive mosquitoes released at experimental sites [35].  
292 Detection of pathogens was demonstrated using i) RT-PCR assays for the presence of viral nucleic  
293 acids and ii) FFA to quantify infectious viral particles directly from mosquito bites. PCR assays  
294 can enable low-cost sampling of pathogens in the field informing community action for disease  
295 prevention. Simultaneously, FFA results provide a window to dynamics of infection transmission  
296 directly through individual mosquito bites, which as of yet remains difficult to study.

297 Currently, ecological distribution of pathogens in our environments is significantly undersampled.  
298 This contributes to dramatic consequences in the form of unexpected viral outbreaks. There is an  
299 urgent need for vector-pathogen sampling to shift from current resource-intensive practices to low-  
300 cost technologies that can perform large-scale surveillance. We hope tools like the *Vectorchip* will  
301 allow us in the future to completely eliminate human-landing catches. The *Vectorchip* provides a  
302 route for multimodal analysis of vector-pathogen dynamics both in lab and field including vector  
303 identification, behavior and pathogen surveillance at a high throughput and resolution. We antici-  
304 pate the use of *Vectorchip* tool can be expanded from vector and pathogen surveillance testing in

305 field sites and lab settings to study of vector biting behavior on chip and expand to other biting  
306 vectors such as ticks and sandflies.

## 307 **Methods**

### 308 **A) Chip fabrication**

309 **a) Main body:** PDMS chips with thickness  $\sim 4$  mm were prepared as the main body of the chip.  
310 Sylgard 184 base and cross linker (Dow Chemicals, USA) were mixed at a 10:1 ratio and cured  
311 at 75 °C on a flat heater surface. Laser ablation ( 60-Watt Mini CO<sub>2</sub> laser, Epiloglaser, USA)  
312 was used to cut holes through the PDMS blocks with desired hole diameter and density. Debris  
313 produced by the laser ablation process was removed using 1 hour sonication in acetone. The chips  
314 were then rinsed with DI water and dried.

315 **b) PDMS membranes:** PDMS membranes were prepared over single side polished, 4 inch silicon  
316 wafers. A layer of positive photoresist (Microposit™ S1813G2) was spun on the wafers to a  
317 thickness of around 2 microns (1500 rpm for 45 s). The resist was softbaked at 80 °C for about  
318 30 minutes. PDMS (Sylgard 184 kit with base and curing agent mixed at 10:1 ratio) was freshly  
319 prepared and spuncoat on top of the wafers. The thickness of the PDMS coat was controlled by  
320 varying the spin speed and time. In order to obtain a membrane with thickness close to 1.6 microns,  
321 PDMS was spun on the wafers at 6500 rpm for 10 minutes. Wafers with thin layers of PDMS were  
322 cured at 70 °C for at least 6 hours. The thickness of the PDMS on the wafers was measured by  
323 cutting strips off of a silicon wafer and measuring the difference in height using a profilometer  
324 (KLA Tencor Alpha Step D500).

325 **c) Vectorchips:** The main body of the chip and wafers with thin PDMS membranes were placed  
326 in a plasma cleaner and exposed to O<sub>2</sub> plasma (80 W, 45 s, 2 sccm O<sub>2</sub> flow). The PDMS chips

327 were then placed in contact with the thin PDMS membranes to enable bonding of the membranes  
328 to the chips. The wafers were baked at 80 °C for around 2 hours to improve the bonding strength.  
329 A razor blade was used to cut outlines around the chips, such that membrane-attached PDMS  
330 chips can detach from the wafers. The wafers were then placed in acetone for approximately 2-4  
331 hours. The sacrificial resist layer is dissolved in acetone and PDMS chips with integrated ultrathin  
332 membrane are separated from silicon wafers. The chips are then rinsed gently in DI water and  
333 dried in an oven.

334 **B) Biting assays:** Vectorchips were hydrophilized by placing in a plasma cleaner (Harrick Plasma)  
335 at high power for 5 mins.

336 In order to test the biting ability of mosquitoes, sugar water was removed from the cages approx-  
337 imately 18 hours prior to the assays. Chips with varying membrane thickness were filled with  
338 defibrinated sheep blood (Hemostat laboratories, USA). The well diameter was kept constant at  
339 1.75 mm. Chips were placed on mosquito cages for approximately 30 minutes, and blood feeding  
340 was monitored visually.

341 For PCR assays, the wells were filled with 10% sucrose solution. Sugar water was removed from  
342 the mosquito cages around 6-18 hours prior to the biting tests. The chips were then placed on  
343 top of a mosquito cage. A strip of tape was adhered on top of the cage and the chip was placed  
344 such that some rows were placed atop the tape and were thus inaccessible for the mosquitoes to  
345 bite through. A heat source (resistive heater or tissue culture flask with warm water) was placed  
346 atop the chips such that their temperature was approximately 37 °C. Mosquitoes bite the chips  
347 for approximately 20-45 minutes, expectorating saliva in the process which is collected in the  
348 wells. A raspberry pi camera attached to the bottom of the cage records mosquito activity on-chip.  
349 After approximately 20-45 minutes, the chips are removed from the cages. Chips bitten by ZIKV  
350 infected mosquitoes were placed on a hotplate set to 98 °C for 15 minutes to inactivate the virus  
351 and facilitate downstream processing.

352 PDMS base (Sylgard 184 part A) and crosslinker (Sylgard 184 part B) were mixed to a weight of  
353 1 gram and placed in a vacuum degasser for removing any bubbles. A glass slide (size: 75 mm ×  
354 50 mm) was taken and approximately 0.75 g of the freshly prepared PDMS was added to the slide.  
355 The PDMS was spread evenly using a pipette tip and was degassed for 2 minutes to remove any  
356 bubbles. The *Vectorchip* used for biting assay was then placed on the slide, membrane-side down  
357 into the thin layer of uncured PDMS carefully.

358 The chip was then dried either at room temperature overnight or in an oven at 80 °C for 20 minutes  
359 (for Zika-infected mosquitoes). This process adheres the chip to a solid glass slide by curing of the  
360 thin PDMS layer and allows the sugar water to evaporate in every well.

361 **C) Mosquito tracking algorithms:** Image recognition algorithms were written in Python 3 see  
362 ref. [21] for details, and used to track mosquito movement on the chip and are available on github  
363 (<https://github.com/felixhol/vectorChip>).

#### 364 **D) RT-PCR assays:**

365 TaqMan™ Fast Virus 1-Step Master Mix was used for the amplification assays. Following primers  
366 and probes were used for the amplification of *Aedes aegypti* mitochondrial DNA and Zika RNA.

367 *Aedes aegypti* Fwd Primer: ACACATGCAAATCACCCATTTC

368 *Aedes aegypti* Rev Primer: CATTGGACAAGGCCTGTA ACT

369 *Aedes aegypti* mtDNA probe: HEX-AGCCCTTGA-ZEN-CCTTTAACAGGAGCT-3IABkFQ

370 Zika virus Fwd Primer: CCGCTGCCCAACACAAG

371 Zika virus Rev Primer: CCACTAACGTTCTTTTGCAGACAT

372 Zika virus probe: FAM-AGCCTACCT-ZEN-TGACAAGCAGTCAGACACTCAA-3IABkFQ

373 The RT-PCR reaction mix was prepared as follows:

374 For every 20 µL of reaction mix:

375 Fast virus mix - 5  $\mu$ L

376 Fwd Primer - 1  $\mu$ L

377 Rev Primer - 1  $\mu$ L

378 Fluorescent probe - 0.5  $\mu$ L

379 DI water - add as required to total 20  $\mu$ L

380 Four  $\mu$ L of reaction mix was pipetted into all wells. Positive control wells were filled with *Aedes*  
381 *aegypti* DNA or Zika virus RNA. Silicone oil (Sylgard 184 part A) was poured over the wells to  
382 prevent against evaporation and allowed to penetrate the wells. If needed, gentle degassing for 15  
383 minutes helped the oil enter the wells. The chips were then placed on a flat-plate thermocycler  
384 (GenePro, Bioer Tech.) and RT-PCR was performed for 42 cycles.

385 50 °C: 10 mins

386 95 °C: 45s

387 cycle  $\times$  42 (95 °C: 35s; 60 °C: 80s)

388 The chips were then scanned using a fluorescence image scanner (Typhoon FLA 9000, GE Health-  
389 care) to obtain the images.

390 qPCR tests (StepOnePLUS, Applied Biosystems) were performed in 96 well plates using identical  
391 samples and conditions as the *Vectorchips* in order to validate the RT-PCR efficiency in the chips.

392 **E) Focus forming assays:** Chips were loaded with DMEM cell culture media in each well and  
393 placed over cages with approximately 50 female Mayaro virus infected *Aedes aegypti* mosquitoes.  
394 The mosquitoes were allowed to bite the chips for 30 minutes. The negative control chips were  
395 bitten by uninfected mosquitoes. Chips were then removed from the cages and 10  $\mu$ L of Vero cell  
396 suspension (1000 cells/ $\mu$ L) was dispensed into each well. To allow the virus particles to adsorb  
397 on to the cell surface, chips were incubated for one hour at 37 °C incubator with 5 % CO<sub>2</sub>. To  
398 remove unbound viral particles, cells were washed once with DMEM without FBS. Thereafter,



399 20  $\mu$ L of 1% methylcellulose (MC) overlay medium supplemented with DMEM and 5% FBS  
400 was added to each well of the chips. Chips were then incubated at 37 °C incubator with 5%  
401 CO<sub>2</sub> for 24 h. Note, to minimize the evaporation rate of culture media from the wells the chips  
402 were incubated in a humidified secondary container. The MC overlay medium was removed, and  
403 cells were fixed with 4% PFA for 20 minutes at room temperature (RT). After the removal of  
404 PFA, cells were washed with 1X PBS. Cell monolayers were then blocked for one hour in PBS  
405 with 3% BSA supplemented with 0.1% TritonX-100. After blocking, monolayers were incubated  
406 with CHIK-48 primary antibody that cross-react with Mayo virus E2 Envelope Glycoprotein (BEI  
407 resources; NR-44002 -1:500) overnight at 4 °C in blocking solution. Unbound primary antibodies  
408 were washed with PBS and incubated with Alexa-488-Conjugated secondary antibody (Invitrogen;  
409 A28175-1:500) for one hour at RT in PBS/3%BSA/0.1%TritonX-100. The secondary antibodies  
410 were removed and washed with PBS. Chips were imaged on an Olympus BX41 epifluorescent  
411 microscope, and foci were quantified.

412 **F) Biological Samples:** The following reagent was provided by Centers for Disease Control and  
413 Prevention for distribution by BEI resources, NIAID, NIH: *Aedes aegypti*, Strain D2S3, Eggs,  
414 NR-45838. The following reagents were obtained through BEI Resources, NIAID, NIH: *Culex*  
415 *tarsalis*, Strain YOLO, Eggs, NR-43026, genomic RNA from Zika Virus, MR 766, NR-50085,  
416 and as part of the WRCEVA program: Mayaro Virus, BeAn343102, NR-49909. A hatching broth  
417 was prepared by grinding 1g of fish food granules (Aqueon goldfish granules) and mixing in 1L  
418 of DI water. The solution was autoclaved and allowed to cool down to room temperature. The  
419 broth was then added to a plastic tray filled with 1L DI water and eggs were hatched in the trays  
420 ( 200 eggs per tray). Ground fish food granules (Aqueon goldfish granules) were provided as  
421 feed for the larvae. The pupae were transferred to cups and placed in polypropylene rearing cages  
422 (Bugdorm, Taiwan). Mosquitoes were reared at 28 °C, 80% humidity with 12 hour light-dark  
423 cycles. Flasks with sugar water (10%) and cotton wicks were placed in the rearing cages for the  
424 mosquitoes. *Aedes aegypti* strain KPPTN, *Aedes albopictus* strain BP, and ZIKV strain FSS13025

425 were provided by Louis Lambrechts (Institut Pasteur). *Aedes aegypti* DNA was obtained using lab  
426 extraction from homogenized, dead mosquitoes.

427 **G) ZIKV infectious blood meal:** Approximately 55 *Aedes aegypti* females (11 days old) housed  
428 in cardboard containers were offered an infectious blood meal of defibrinated sheep blood supple-  
429 mented with Zika virus at  $1 \times 10^7$  FFU/mL using a hemotek blood feeder. Females were allowed  
430 to feed for 15 minutes and subsequently cold anesthetized to separate fed and non-fed individu-  
431 als. Infected adults were maintained at 28C and 80% humidity having continuous access to a 10%  
432 sugar solution. Experiments were performed at 17 and 18 days post infection.

433 **H) Fluorescent saliva imaging:** To facilitate imaging of fluorescent saliva, *Ae. aegypti* were  
434 allowed to feed on a solution containing 0.4% rhodamine B and 10% sucrose in water for at least  
435 48 hours. The rhodamine B ingested during sugar feeding stains the mosquito body including  
436 saliva. [36] Imaging was performed using the biteOscope as described previously [21] with the  
437 following adjustments: A 532 nm, 5 mW laser (Sparkfun, COM-09906) was used for illumination,  
438 and a 550 nm longpass filter (Thorlabs FEL0550) was used as an emission filter. Fluorescent saliva  
439 droplets on vectorchips were quantified by scanning the chips before and after the biting assays on  
440 Typhoon FLA 9000 gel scanner.

## 441 **Acknowledgements**

442 This project was supported by grants from United States Agency for International Development  
443 (USAID) and National Institute of Health (NIH). Part of this work was performed at the Stanford  
444 Nano Shared Facilities (SNSF), supported by the National Science Foundation under award ECCS-  
445 1542152, at Stanford University.

446 We thank Louis Lambrechts (Insect Virus Interactions Unit, Institut Pasteur, Paris, France) and

447 Lark Coffey (School of Veterinary Medicine, University of California, Davis, CA, USA) for pro-  
448 viding access to arbovirus laboratories. USAID, CDC, SNF, NIH, BEI.

449 FJHH was supported by a Rubicon fellowship for the Netherlands Foundation for Scientific Re-  
450 search, a Career Award at the Scientific Interface from the Burroughs Wellcome Fund, and a Marie  
451 Curie Fellowship from the European Union.

452 SP and JLR were supported by NIH Grants R01AI128201, R01AI150251, R01AI116636, USDA  
453 Hatch funds (Accession #1010032; Project #PEN04608), and a grant with the Pennsylvania De-  
454 partment of Health using Tobacco Settlement Funds.

## 455 **References**

456 [1] Organization, W. H. Global vector control response 2017-2030. Tech. Rep., Geneva, Switzer-  
457 land (2017).

458 [2] Kraemer, M. U. *et al.* Past and future spread of the arbovirus vectors *aedes aegypti* and *aedes*  
459 *albopictus*. *Nature microbiology* **4**, 854–863 (2019).

460 [3] Li, R. *et al.* Climate-driven variation in mosquito density predicts the spatiotemporal dynam-  
461 ics of dengue. *Proceedings of the National Academy of Sciences* **116**, 3624–3629 (2019).

462 [4] Tangena, J.-A. A., Thammavong, P., Hiscox, A., Lindsay, S. W. & Brey, P. T. The human-  
463 baited double net trap: an alternative to human landing catches for collecting outdoor biting  
464 mosquitoes in lao pdr. *PLoS One* **10**, e0138735 (2015).

465 [5] Kenea, O. *et al.* Comparison of two adult mosquito sampling methods with human landing  
466 catches in south-central ethiopia. *Malaria journal* **16**, 30 (2017).

- 467 [6] Service, M. W. *Mosquito Ecology: Field Sampling Methods* (Applied Science Publishers,  
468 1976).
- 469 [7] Ndebele, P. & Musesengwa, R. Ethical dilemmas in malaria vector research in africa: making  
470 the difficult choice between mosquito, science and humans. *Malawi Medical Journal* **24**, 65–  
471 68 (2012).
- 472 [8] Achee, N. L., Youngblood, L., Bangs, M. J., Lavery, J. V. & James, S. Considerations for the  
473 use of human participants in vector biology research: a tool for investigators and regulators.  
474 *Vector-Borne and Zoonotic Diseases* **15**, 89–102 (2015).
- 475 [9] James, S., Takken, W., Collins, F. H. & Gottlieb, M. Needs for monitoring mosquito trans-  
476 mission of malaria in a pre-elimination world. *The American Journal of Tropical Medicine*  
477 *and Hygiene* **90**, 6–10 (2014).
- 478 [10] Dubrulle, M., Mousson, L., Moutailler, S., Vazeille, M. & Failloux, A.-B. Chikungunya virus  
479 and aedes mosquitoes: saliva is infectious as soon as two days after oral infection. *PloS one*  
480 **4**, e5895 (2009).
- 481 [11] Schmid, M. A., Kauffman, E., Payne, A., Harris, E. & Kramer, L. D. Preparation of mosquito  
482 salivary gland extract and intradermal inoculation of mice. *Bio-protocol* **7** (2017).
- 483 [12] Vogt, M. B. *et al.* Mosquito saliva alone has profound effects on the human immune system.  
484 *PLoS neglected tropical diseases* **12**, e0006439 (2018).
- 485 [13] Hall-Mendelin, S. *et al.* Exploiting mosquito sugar feeding to detect mosquito-borne  
486 pathogens. *Proceedings of the National Academy of Sciences* **107**, 11255–11259 (2010).
- 487 [14] Girod, R. *et al.* Detection of chikungunya virus circulation using sugar-baited traps during a  
488 major outbreak in french guiana. *PLoS neglected tropical diseases* **10**, e0004876 (2016).

- 489 [15] Fontaine, A., Jiolle, D., Moltini-Conclois, I., Lequime, S. & Lambrechts, L. Excretion of  
490 dengue virus rna by aedes aegypti allows non-destructive monitoring of viral dissemination  
491 in individual mosquitoes. *Scientific reports* **6**, 1–10 (2016).
- 492 [16] Ramírez, A. L. *et al.* Mosquito excreta: A sample type with many potential applications  
493 for the investigation of ross river virus and west nile virus ecology. *PLoS neglected tropical*  
494 *diseases* **12**, e0006771 (2018).
- 495 [17] Pilotte, N. *et al.* Laboratory evaluation of molecular xenomonitoring using mosquito and  
496 tsetse fly excreta/feces to amplify plasmodium, brugia, and trypanosoma dna. *Gates Open*  
497 *Research* **3** (2019).
- 498 [18] Grubaugh, N. D. *et al.* Mosquitoes transmit unique west nile virus populations during each  
499 feeding episode. *Cell reports* **19**, 709–718 (2017).
- 500 [19] Deng, L. *et al.* A novel mosquito feeding system for routine blood-feeding of aedes aegypti  
501 and aedes albopictus. *Trop Biomed* **29**, 169–74 (2012).
- 502 [20] Costa-da Silva, A. L. *et al.* Glytube: a conical tube and parafilm m-based method as a  
503 simplified device to artificially blood-feed the dengue vector mosquito, aedes aegypti. *PLoS*  
504 *one* **8**, e53816 (2013).
- 505 [21] Hol, F. J., Lambrechts, L. & Prakash, M. Biteoscope, an open platform to study mosquito  
506 biting behavior. *eLife* **9**, e56829 (2020).
- 507 [22] Xia, Y. & Whitesides, G. M. Soft lithography. *Annual review of materials science* **28**, 153–  
508 184 (1998).
- 509 [23] Duffy, D. C., McDonald, J. C., Schueller, O. J. & Whitesides, G. M. Rapid prototyping of  
510 microfluidic systems in poly (dimethylsiloxane). *Analytical chemistry* **70**, 4974–4984 (1998).

- 511 [24] Leclerc, E., Sakai, Y. & Fujii, T. Cell culture in 3-dimensional microfluidic structure of pdms  
512 (polydimethylsiloxane). *Biomedical microdevices* **5**, 109–114 (2003).
- 513 [25] Shin, Y. S. *et al.* Pdms-based micro pcr chip with parylene coating. *Journal of Micromechan-*  
514 *ics and Microengineering* **13**, 768 (2003).
- 515 [26] Ramasubramanian, M., Barham, O. & Swaminathan, V. Mechanics of a mosquito bite with  
516 applications to microneedle design. *Bioinspiration & biomimetics* **3**, 046001 (2008).
- 517 [27] Kong, X. & Wu, C. Mosquito proboscis: An elegant biomicroelectromechanical system.  
518 *Physical Review E* **82**, 011910 (2010).
- 519 [28] Ribeiro, J. M., Martin-Martin, I., Arca, B. & Calvo, E. A deep insight into the sialome of  
520 male and female aedes aegypti mosquitoes. *PloS one* **11**, e0151400 (2016).
- 521 [29] Schneider, B. S. & Higgs, S. The enhancement of arbovirus transmission and disease by  
522 mosquito saliva is associated with modulation of the host immune response. *Transactions of*  
523 *the Royal Society of Tropical Medicine and Hygiene* **102**, 400–408 (2008).
- 524 [30] Aubry, F. *et al.* Enhanced zika virus susceptibility of globally invasive aedes aegypti popula-  
525 tions. *Science* **in press** (2020).
- 526 [31] Takahashi, M. The effects of environmental and physiological conditions of culex tritaen-  
527 niorhynchus on the pattern of transmission of japanese encephalitis virus. *Journal of medical*  
528 *entomology* **13**, 275–284 (1976).
- 529 [32] Hoffmann, A. A. *et al.* Successful establishment of wolbachia in aedes populations to sup-  
530 press dengue transmission. *Nature* **476**, 454–457 (2011).
- 531 [33] Aliota, M. T., Peinado, S. A., Velez, I. D. & Osorio, J. E. The wmel strain of wolbachia  
532 reduces transmission of zika virus by aedes aegypti. *Scientific reports* **6**, 28792 (2016).

533 [34] Long, K. C. *et al.* Experimental transmission of mayaro virus by aedes aegypti. *The American*  
534 *journal of tropical medicine and hygiene* **85**, 750–757 (2011).

535 [35] Gantz, V. M. *et al.* Highly efficient cas9-mediated gene drive for population modification of  
536 the malaria vector mosquito anopheles stephensi. *Proceedings of the National Academy of*  
537 *Sciences* **112**, E6736–E6743 (2015).

538 [36] Johnson, B. J. *et al.* Use of rhodamine b to mark the body and seminal fluid of male aedes ae-  
539 gypti for mark-release-recapture experiments and estimating efficacy of sterile male releases.  
540 *PLOS Neglected Tropical Diseases* **11**, e0005902 (2017).

## 541 Figures and Captions

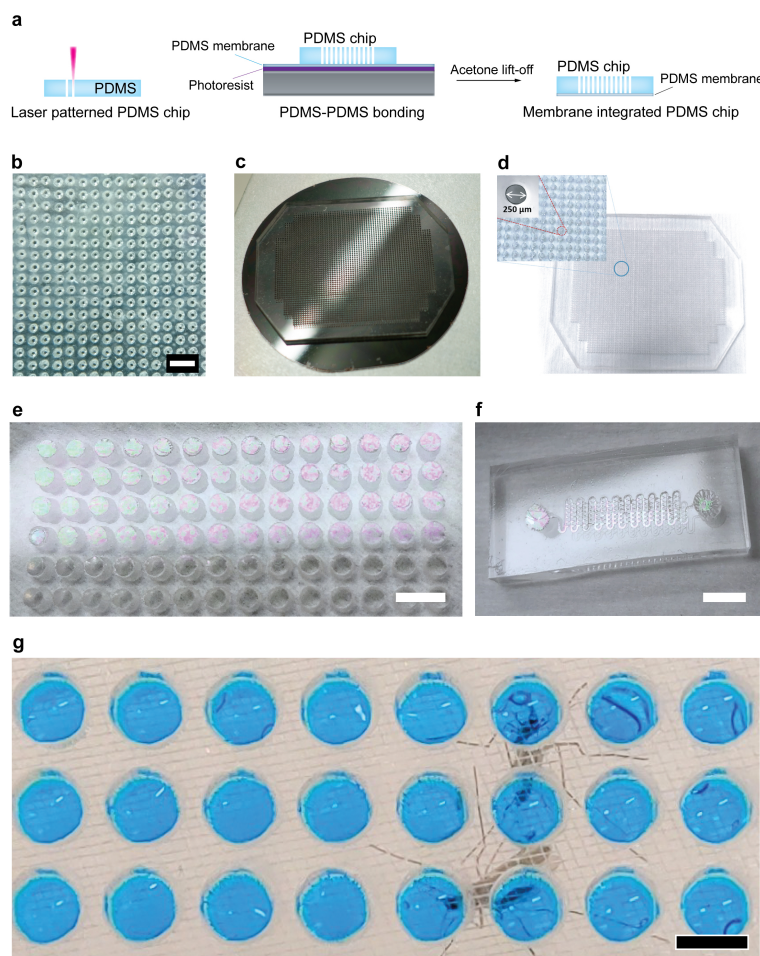
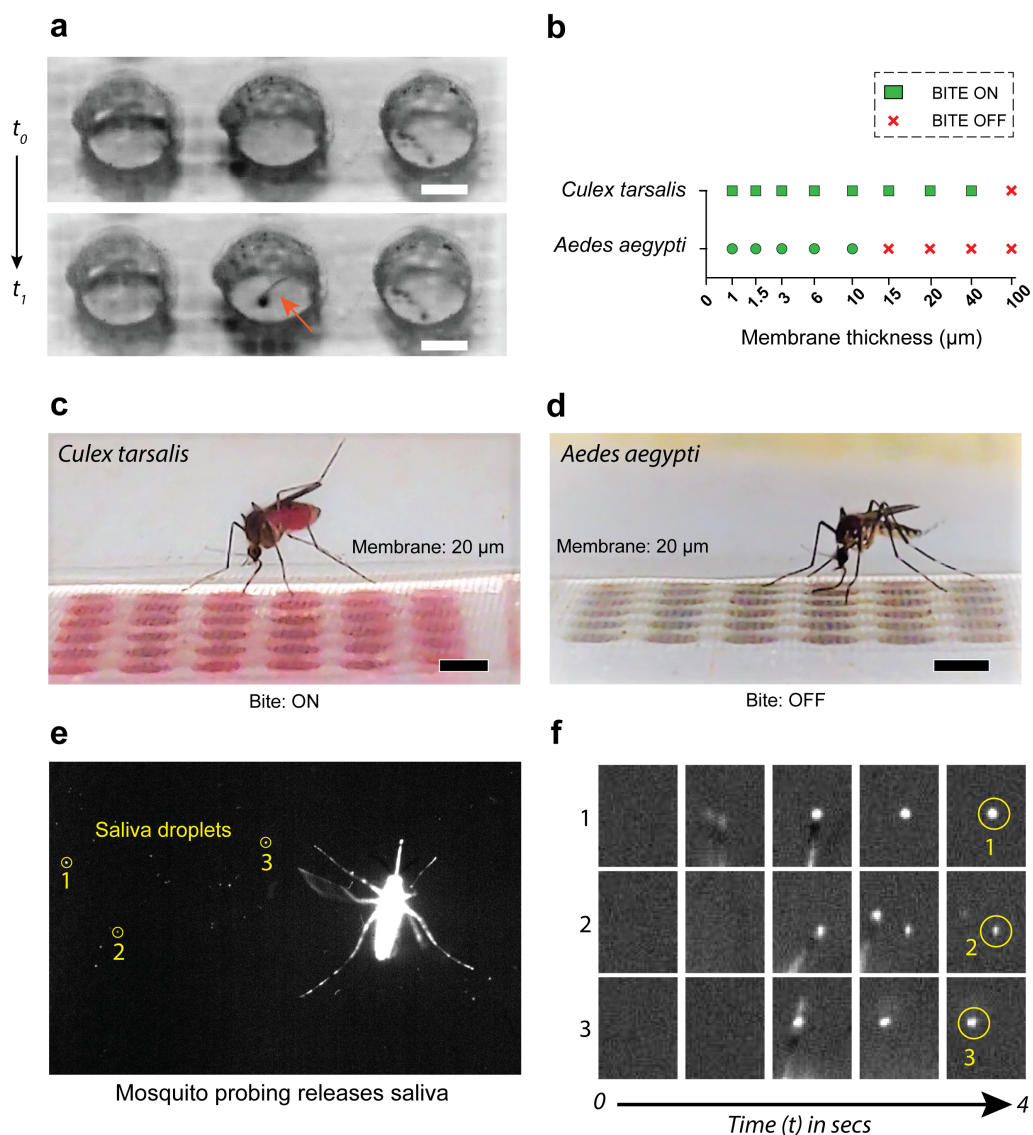
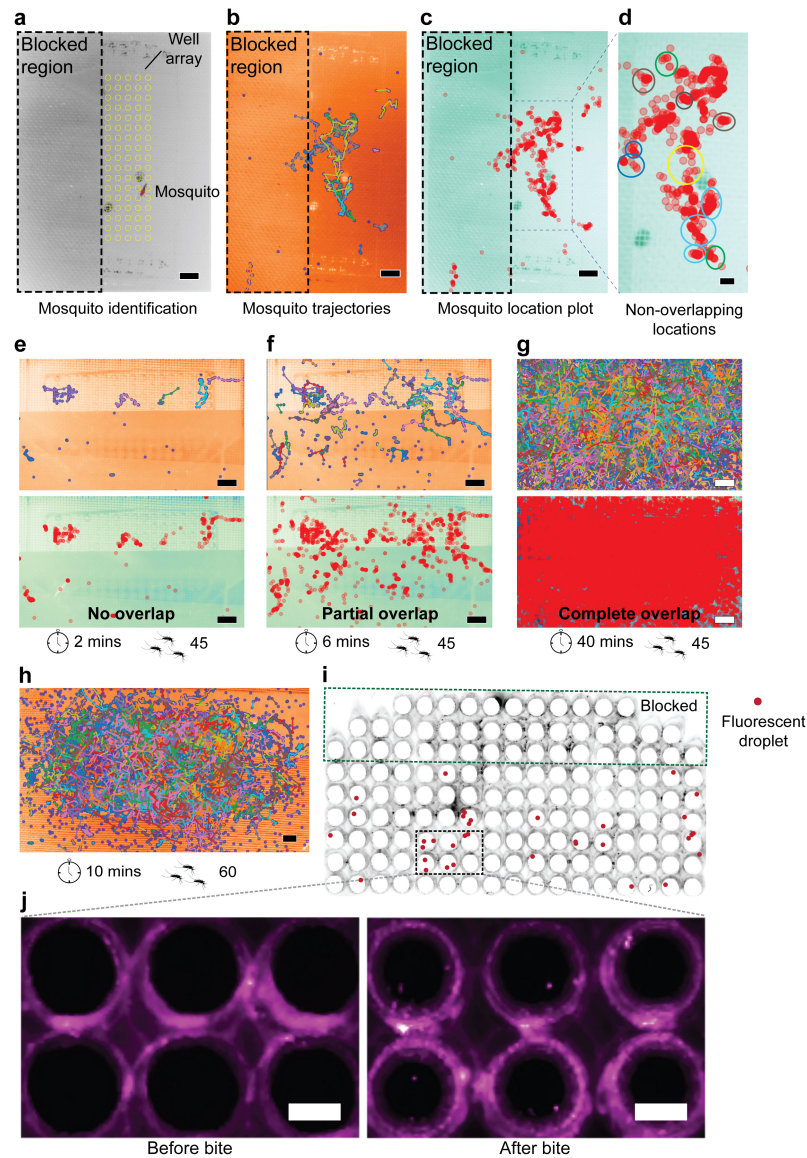


Figure 1: **Fabrication of *Vectorchips* for collection of mosquito saliva and molecular assays.** a) Schematic showing the fabrication process of *Vectorchips*. Laser patterning is used to obtain through-holes in blocks of PDMS. A thin sacrificial layer of photoresist is spread onto a silicon wafer followed by spin-coating a thin film of PDMS on the wafer surface. The laser-patterned body of the chip is then bonded to the thin film of PDMS using plasma activated PDMS-PDMS bonding. Membrane-bonded chips are obtained by placing the wafer in an acetone bath, where the sacrificial layer of resist is dissolved. (b) A PDMS block with laser-generated through-holes (diameter 250  $\mu\text{m}$ ). (c) A PDMS chip bonded to a 1.6  $\mu\text{m}$  thin PDMS membrane on a 4 inch silicon wafer. (d) A *Vectorchip* with around 3000 wells (dia: 250  $\mu\text{m}$ ) is shown. (e) Chip with well diameter 1.75 mm and a visible PDMS membrane (thickness 1.6  $\mu\text{m}$ ). (f) Design fluidity in fabrication allows production of channel-integrated chips with a PDMS membrane on top. (g) These wells can be loaded with feeding solution, reaction reagents, and can store mosquito saliva after biting assays. Wells loaded with feeding media (10% sucrose laced with blue food color) shown here. Scale bars represent 1 mm in (b), 5 mm in (e), and 2 mm in (f, g).





**Figure 2: Mosquito biting on Vectorchips.** (a) Stylet entry through a PDMS membrane for an *Aedes aegypti* female. (b) Mosquito feeding success as a function of membrane thickness for two mosquito species - *Aedes aegypti* and *Culex tarsalis*. We demonstrate that by tuning the membrane thickness we can turn biting “on” or “off”. Biting “off” is defined as when no mosquito in the cage was able to feed from the chip in a duration of 30 minutes. (c) A *Culex tarsalis* female mosquito biting through a 20  $\mu\text{m}$  thick PDMS membrane. (d) Bending of the proboscis observed for an *Aedes aegypti* female, indicating failure in biting through the 20  $\mu\text{m}$  membrane. (e) Fluorescent salivary droplets expectorated by an *Aedes aegypti* mosquito while probing. These mosquitoes were fed on rhodamine-laced sugar water resulting in fluorescent saliva. (f) Timelapse images show a magnified view of fluorescent salivary droplet deposition over a period of 4 seconds. Scale bars represent 500  $\mu\text{m}$ s in (a) and 2 mm in (c, d).



**Figure 3: Tracking mosquito activity on chip.** (a) Image recognition software is used to identify and track mosquitoes on the chip. Wells are highlighted in yellow. (b) Trajectories of mosquito movement can be plotted and indicate the overlap between different movement tracks. (c) Location plot of mosquitoes on the chip indicated by red circles. Regions with overlapping red circles are darker in color. (d) Trajectory and location plot can be used in combination to identify regions with individual mosquito locomotion activity as compared to regions with more crowding. (e-g) Varying experimental parameters (time of biting shown here) can be used to obtain either individual mosquito plots or population data. Three cases are discussed where there is (e) no overlap between multiple probing trajectories, (f) partial overlap and (g) complete overlap. (h-j) Tracking and corresponding salivary droplet deposition data for a chip. (h) shows extensive translocation activity of mosquitoes on chip. (i, j) Several wells show single fluorescent droplet indicating probing by a single mosquito, whereas other wells show multiple probe marks. The tracking and probing data suggest that we should be able to obtain both individual bite data as well as multi-bite statistics on *Vectorchip*. Scale bars represent 5 mm in (a-c, e-h), 2 mm in (d), and 1 mm in (j).

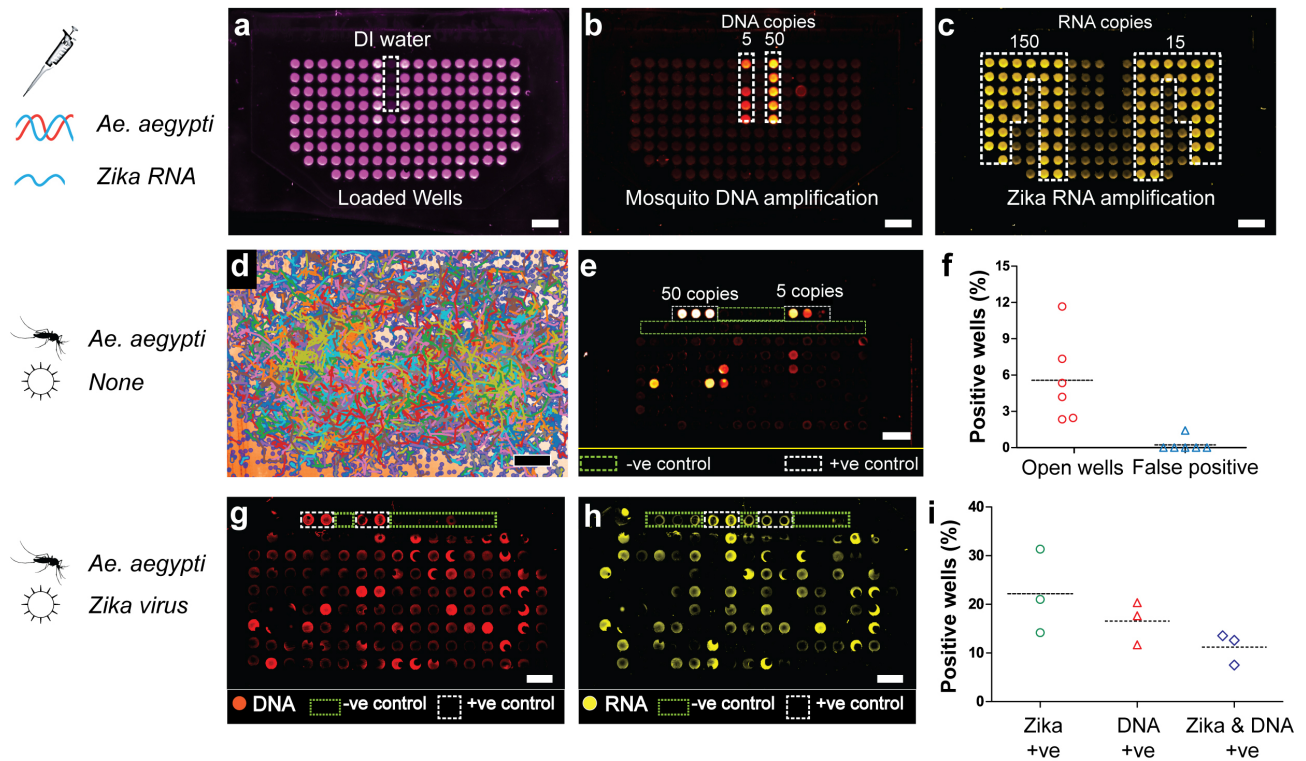


**Figure 4: On-chip PCR for detection of mosquito and pathogen** (a-c) A spiked assay demonstrates successful amplification of *Aedes aegypti* DNA and Zika RNA on chip. (a) indicates wells filled with PCR mix, with ROX dye providing the background fluorescence. Fluorescent wells indicate amplification of (b) mosquito DNA, and (c) Zika RNA on chip. Assays were performed with uninfected mosquitoes where (d) tracking patterns were collected and demonstrate extensive translocation activity on the chip. (e) PCR shows detection of mosquito DNA on the chip directly from biting. (f) Percentage of wells available for biting on *Vectorchip* that display a positive PCR outcome. The false positive rate (amplification in wells that were covered by tape) was close to zero (0.23%). Assays performed with Zika infected mosquitoes indicate presence of both (g) *Aedes aegypti* DNA and (h) Zika virus RNA after bites on chip. (i) Percentage of wells available for biting that show a positive signature for Zika RNA, mosquito DNA or both. Scale bars represent 5 mm in (a-e) and 2 mm in (g, h).

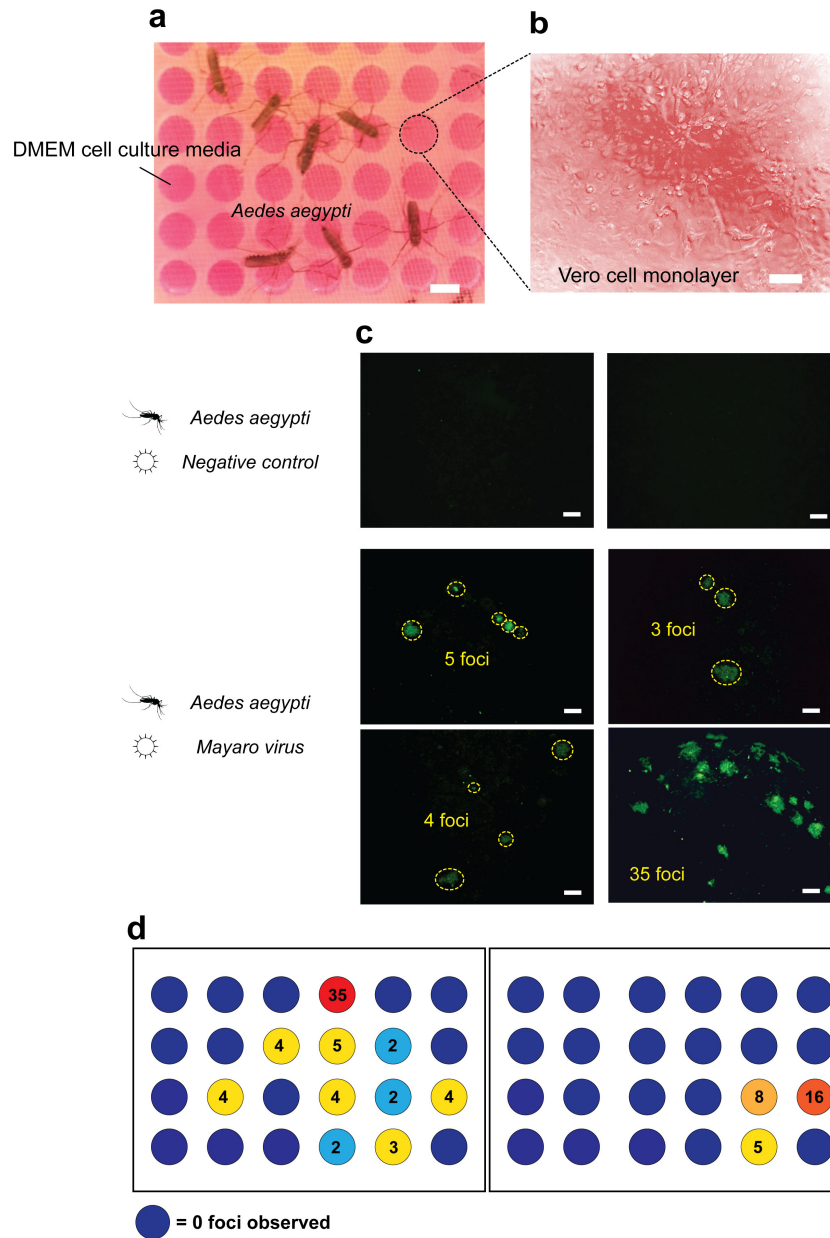


**Figure 5: Quantifying active viral particles using focus forming assays.** Focus forming assays on *Vectorchips* can directly quantify the number of active viral particles in mosquito bites, without the need for isolation of individual mosquitoes and manual salivary extraction. (a) Image shows *Aedes aegypti* mosquitoes infected with Mayaro virus biting on *Vectorchips* filled with DMEM cell culture media. (b) A monolayer of vero cells growing on *Vectorchip* membrane. (c) FFA performed on a *Vectorchip*. Control samples and compartments with active Mayaro virus are shown. Green channel shows fluorescence from an antibody against a viral envelope protein. Every green island represents an active viral particle. No active viral particles were seen in the control wells. (d) FFA formed on two chips and viral foci were counted using the antibody fluorescence. Scale bars represent 2 mm in (a), 30  $\mu$ m in (b) and 100  $\mu$ m in (c).